Diurnal rhythmicity in metabolism and salivary effector expression shapes host colonization by aphids

Jinlong Han[1], Daniel Kunk[1,2], Meihua Cui[1], Yoshiahu Goldstein[3], Vered Tzin[3] and Vamsi J. Nalam[1,2*]

[1]Department of Agricultural Biology, Colorado State University, Fort Collins, CO, USA

[2]Department of Cell and Molecular Biology, Colorado State University, Fort Collins, CO, USA

[3]French Associates Institute for Agriculture and Biotechnology of Drylands, Jacob Blaustein Institutes for Desert Research, Ben-Gurion University of the Negev, Midreshet Ben Gurion, Israel

***Corresponding Author:** Vamsi.Nalam@colostate.edu

Keywords:

Diurnal rhythms, aphids, feeding behaviors, salivary effectors, osmoregulation.

Abstract

Diurnal rhythms influence insect behavior, physiology, and metabolism, optimizing their performance by adapting to daily changes in the environment. While their impact on agricultural pests has been briefly explored, our understanding of how these rhythms drive adaptative responses in pest biology and influence host colonization remains elusive. Here, we show that a notorious global aphid pest, *Rhopalosiphum padi*, exhibits distinct diurnal patterns in feeding behavior, with elevated honeydew excretion at night and extended phloem salivation during early nighttime. Temporal aphid transcriptome profiling reveals four diurnally rhythmic clusters, two of which peak at night, exhibiting enrichment in carbohydrate and amino acid metabolism. Beyond the established role in manipulating host responses and allowing sustained feeding, our study reveals the first evidence in any insect species for cyclical fluctuations in salivary effector expression. Silencing key effector genes, peaking in expression during the increased nighttime salivation, results in a more pronounced reduction in aphid feeding activity on host plants during the night compared to the day, a phenomenon not observed on artificial diets. A better understanding of aphid diurnal rhythms and their roles on host colonization provides a promising avenue to refine and optimize pest management, granting a strategic advantage for minimizing crop damage.

Introduction

The recurring cycles of day and night caused by Earth's daily rotation profoundly influence all life, including plants and their pests. All living organisms have evolved internal biological clocks (i.e., circadian clocks) to anticipate and respond to cyclical changes in their environments by orchestrating various behavioral and physiological processes [1]. Diurnal and circadian rhythms entail daily biological cycles, with circadian rhythms representing a subset characterized by internally sustained oscillations that persist in the absence of external cues [2]. Our understanding of these rhythms has led to profound insights into mechanisms governing the intricate biological processes that shape various daily and seasonal behavioral patterns in diverse taxa, including insects and plants. Despite a significant body of knowledge on diurnal rhythms in model organisms and host-parasite interactions [3,4], research on agricultural pests and their interactions with plant hosts remains underexplored. Given the significant threat pests pose to crop production, deciphering the temporal aspects of their behavior, physiology, and gene expression is a crucial step toward developing more effective pest control strategies [5,6].

Aphids are among the most devastating pests worldwide, causing significant damage to various economically important crops through their consumption of sugar-rich phloem sap, delivery of phytotoxic salivary secretions, transmission of plant-pathogenic viruses, and promoting the growth of sooty-mold on their sugar-rich excrement [7]. Studies on circadian clock-regulated plant defenses against arthropod pests reveal that pests strategically anticipate and exploit plant rhythms. For example, the cabbage looper (*Trichoplusia ni*), a generalist herbivore, shows rhythms in feeding, with peak feeding occurring during the latter part of the day [8]. Conversely, cell-content feeders like spider mites (*Tetranychus urticae*) exploit a nighttime "lull" in jasmonate-induced defenses, causing more damage during the night [9]. Given that aphids rely entirely on acquiring phloem sap from plants for their reproduction and survival, they likely need to anticipate, respond to, and counteract the challenges posed by daily rhythms in their hosts. Notably, green peach aphids (*Myzus persicae*) feeding on Arabidopsis plants exhibit peak honeydew droplet excretion during the day [10]. These diurnal patterns in aphids extend beyond honeydew excretion, encompassing aspects such as locomotion, larviposition, sex hormone release, egg hatching, and feeding [11–16]. While these studies have begun to broaden our understanding of aphid diurnal rhythms, our knowledge about how aphids regulate their rhythmic behaviors and interact with their hosts over daily cycles is lacking.

The high energy demand for aphid reproduction and the 'nitrogen and sugar barrier' in phloem sap necessitate aphids to feed incessantly from their host plants [17,18]. To facilitate this continuous feeding, aphids synthesize watery saliva in their salivary glands and secrete it into plant cells. This watery saliva comprises a complex blend of proteins with enzymatic activity, including cell-wall degrading enzymes, proteases, polyphenol oxidases, oxidoreductases, and peroxidases, as well as diverse calcium-binding proteins, and many others with unknown functions [19]. Collectively termed effectors, these salivary proteins modify plant defense and physiology to better facilitate aphid feeding, survival, and reproduction [20]. With the advancement in omics technologies, numerous salivary effector candidates have been identified in several aphid species [21–23]. An early and renowned example is C002, a protein with an unknown function

that is essential for continuous feeding from sieve elements [24]. Silencing C002 expression results in lethal outcomes in the pea aphid, *Acyrthosiphon pisum*, and diminished fecundity in the green peach aphid, *Myzus persicae* [25,26]. Despite the pivotal roles of salivary effectors in the aphid colonization of host plants, knowledge about whether their expression or function undergoes diurnal rhythms is unknown.

Another consequence of a sugar-rich diet is that aphids must process and excrete excess sugar to maintain an appropriate osmotic balance [18]. Aphid osmoregulation involves physiological processes such as the breakdown of sucrose into glucose and fructose, their polymerization and expulsion as honeydew, and the rapid cycling of water between the midgut and hindgut [27,28]. Additionally, aphids feed during the night when phloem sugar content is lower [16] and occasionally drink dilute sap from the xylem, a behavior hypothesized to contribute to rehydration [29]. At the molecular level, several genes involved in osmoregulation have been identified in aphids, and their silencing has been shown to elevate osmotic pressure in aphid hemolymph and impair performance [30–32]. A prior study also showed periodic variations in the expression of osmoregulatory genes throughout a 24 h period in the bird cherry-oat aphid, *Rhopalosiphum padi* [16]. Although diurnal fluctuation in phloem sap composition and its impact on aphid performance has been reported [33–36], an in-depth investigation into diurnal variation of aphid osmoregulation at the behavioral and molecular level is currently lacking.

Here, our study shows the diurnal rhythmicity of feeding behavior and gene expression in *R. padi*, a serious global pest of cereals, and its implications for aphid-host interactions [37]. We demonstrate diurnal variations in honeydew excretion and specific feeding activities, notably the salivation process into the phloem. Our temporal analysis of the aphid transcriptome reveals diurnally rhythmic gene clusters with unique expression patterns and pathway enrichment, rationalizing the observed diurnal changes in our aphid feeding assays. Significantly, diurnally rhythmic putative salivary effectors were identified, with many showing peak expression during the increased nighttime salivation. By integrating behavioral and molecular experiments, we unveil a significant time-oriented role of osmoregulatory and salivary effector genes in aphids feeding on host plants. These findings provide novel insights into the diurnal regulation of aphid behavior, metabolism, and salivary effectors, highlighting their crucial roles in colonizing host plants.

Results

Diurnal rhythmicity in *R. padi* feeding behaviors.

Diurnal variation of honeydew excretion in *R. padi* was investigated under a 12L:12D cycle for 48 h on wheat plants. Our study found that the number of honeydew droplets produced per aphid was higher during nighttime (12.09 ± 0.75, mean ± standard error of mean) as opposed to daytime (8.42 ± 0.57) (Fig. 1a). The experiment was repeated on an artificial diet to determine if the observed patterns were independent of plant-derived cues. Although fewer honeydew droplets were produced on the diet overall, a higher number of honeydew droplets was

consistently produced per aphid on the diet during the night (0.23 ± 0.05) compared to the day (0.09 ± 0.03) (Fig. 1b).

The diurnal feeding behavior of *R. padi* was further elucidated using the electrical penetration graph (EPG) technique by measuring feeding at 4 h intervals over a 24 h period (12L:12D). Significant differences were observed in various aphid feeding activities over each timepoint (Supplementary Data 1), including the phloem salivation (E1) phase. Adult *R. padi* spent the longest time in E1 between 12-16 zeitgeber time (zt, refers to an environmental agent or event that provides the stimulus to set or reset a biological clock) and the shortest time between 0-4zt, each of which represents the time period directly following the removal or introduction of the light cues, respectively (Fig. 1c). We also identified a diurnal rhythm in the total duration of E1, with an acrophase (the estimated time in a rhythmic cycle when a peak or maximum value occurs) occurring at 9.8zt (Fig. 1c, Supplementary Table 1). Interestingly, despite the higher honeydew excretion at night (Fig. 1a), the total time spent in phloem ingestion (E2 phase) did not differ over the 24 h period. No diurnal rhythm was detected for the E2 phase (Fig. 1d). Therefore, we hypothesize that the observed day-night variations in salivation and honeydew excretion are associated with diurnally regulated genes involved in the expression of salivary effectors and metabolic pathways linked to aphid feeding, such as osmoregulation.

Temporal gene expression patterns in *R. padi* reveal diurnal rhythmicity.

Temporal transcriptome profiles were collected from *R. padi* whole bodies over a 24 h period to identify diurnal rhythms in gene expression. A total of 49,486 transcripts were assembled with an average sequence length of 2,204 bp. The overall read mapping rate against the *R. padi* reference genome and Benchmarking Universal Single-Copy Orthologs (BUSCO) score for complete sequences were 97% and 99%, respectively (Supplementary Table 2). Of the total assembled transcripts, 4,460 (9.2%) showed significant diurnal rhythmicity over a 24 h period (Supplementary Data 2). 2,913 and 1,547 rhythmic transcripts were identified to have acrophases during the day (0-12zt) and night (12-24zt), respectively. Most transcripts displayed acrophases between 4-8zt and 17-19zt, representing midday and midnight periods, respectively (Fig. 2a).

Soft-clustering analysis classified rhythmic transcripts into four discrete clusters (Fig. 2b). Of the total rhythmic transcripts, 95% were clustered, with 1288, 431, 1143, and 1388 sequences assigned to clusters 1, 2, 3, and 4, respectively (Supplementary Data 3). Most rhythmic transcripts in clusters 1 and 4 showed acrophases during the day at ~4-5zt and ~6-8zt. Cluster 2, containing the least number of transcripts (10% of clustered rhythmic transcripts), was represented by sequences with acrophases occurring during the late night-early morning transition (~21-1zt). Cluster 3 was mainly represented by transcripts with acrophases during the night at ~16-20zt.

Pathway enrichment analysis showed that cluster 1 was enriched in the pathways for the spliceosome, DNA replication, and basal transcription factors (Fig. 2c, Supplementary Data 3), indicating the active regulation of mRNA and protein production during the day. Cluster 2 did not show significant pathway enrichment but exhibited significant gene ontology (GO) terms

related to small molecule, lipid, and carbohydrate metabolic processes (Supplementary Fig. 1). Cluster 3 displayed enrichment in pathways associated with lysosome and various biochemical processes involved in starch, sugar, nitrogen, and amino acid metabolism, indicating higher night-time carbohydrate and amino acid metabolic activities in aphids. Cluster 4 was notably enriched in pathways related to purine metabolism, thiamine metabolism, and multiple pathways associated with human neurodegenerative diseases.

Silencing diurnally rhythmic osmoregulatory genes impacts aphid performance.

Osmoregulation is an important physiological activity to tolerate sugar-rich phloem sap during aphid feeding. Three osmoregulatory genes, *aquaporin 1* (AQP1) [31], *gut sucrase 1* (SUC1) [30,38,39], and *gut sugar transporter 4* [40], were previously reported to display diurnal patterns in *R. padi* [16]. In our study, all three genes were confirmed to be diurnally rhythmic, with acrophases occurring at 15-22zt (Fig 2d-e, Supplementary Table 3). To determine whether the osmoregulatory genes contributed to diurnal variations in honeydew excretion, AQP1, and SUC1 were silenced by injecting aphids with dsRNA targeting each gene. A significant silencing of AQP1 and SUC1 was confirmed 24 hours post-injection (hpi) (Supplementary Fig. 2a-b) with a knockdown efficiency of 44% and 50%, respectively. Silencing AQP1 and SUC1 increased aphid mortality over time, and reduced nymph production by 31% and 66% at 96 hpi, respectively (Fig. 2f-g). Moreover, silencing the two genes markedly reduced honeydew excretion and abolished rhythms in the number of honeydew droplets produced by aphids between the day and night (Fig. 2h). This affirms their significant roles in the diurnal regulation of honeydew excretion and osmoregulation.

Diurnal rhythmicity in *R. padi* salivary effectors.

Given the observed diurnal rhythm in the E1 salivation phase, we sought to determine the presence of diurnal rhythms in the expression of aphid salivary effectors. Previously, 156 genes were identified as putative salivary effectors in *R. padi* [23]. Our study retrieved 93% of putative effectors (145 genes represented by 264 transcripts) by searching all transcripts against the *R. padi* putative effector dataset (Supplementary Data 4). Among them, 42 exhibited diurnal rhythmicity, with 28 exhibiting acrophases at 6-8zt during the day and 14 with acrophases at 18-19zt and 22-23zt at night (Fig. 3a, Supplementary Table 4).

The expression levels of these rhythmic putative effectors were further examined in *R. padi* heads compared to the bodies (body samples excluded tissue from heads and unborn nymphs). We confirmed that the expressions of all rhythmic putative effectors were significantly higher in the heads, except for the putative effector MSTRG.15390.2, which lacked assigned count values across head and body samples (Supplementary Fig. 3). Hierarchical clustering of the rhythmic putative effectors identified four main clades, each showing distinct times of peak expression (Fig. 3a). Transcripts in clades 1 and 2 peaked in expression at the transition from day to night and the early portion of mid-day, respectively. In contrast, transcripts within clade 3

193 exhibited peak expressions at the end of the night and early morning, while clade 4 consisted of
194 transcripts with expression peaking towards the end of the night. Notably, 43% of rhythmic
195 putative effectors with peak expressions occurring at 12-16zt in clade 1 and 4 coincided with the
196 timing of increased E1 salivation, including a well-characterized salivary effector - C002
197 (AphidBase accession - g12266.t1).

198 GO enrichment analysis highlighted two significantly enriched terms for all putative
199 effectors: extracellular region and chitin-binding (Fig. 3b). The former supports a secretory role
200 for these effectors, and the latter implies their potential time-dependent functions in evading or
201 interfering with chitin-triggered plant immunity [41,42]. These findings provide evidence of diurnal
202 rhythms in salivary effector expression, with a subset peaking in expression at the same time as
203 increased nighttime salivation. It also suggests that different blends of salivary effectors are
204 secreted into the plants at different times of the day and represents the first report of diurnal
205 rhythmicity in salivary effector gene expression in any aphid species.

206

207 **Key salivary effectors identified for functional analysis.**

208 To elucidate the functions of diurnally rhythmic salivary effectors in aphid-plant interactions, we
209 selected C002 and a novel effector, E8696 (AphidBase accession - g8696.t1), based on their high
210 amplitude values (i.e. half the difference between the highest and lowest points of a rhythmic
211 cycle), positioning them among the top five compared to other rhythmic putative effectors (Fig.
212 4a, Supplementary Table 4). According to our soft-clustering analysis, C002 and E8696 were
213 assigned to cluster 3 with membership scores of 0.895 and 0.979, respectively (Supplementary
214 Data 3). Their high membership scores designate them as core members within the cluster [43].
215 Additionally, both genes also showed significantly higher expression in *R. padi* heads compared
216 to bodies (Fig. 4b) and peaked in expression at 16zt (midnight) (Fig. 3c-d).

217 Sequence analysis revealed that E8696 encodes for a protein of unknown function with a
218 predicted signal peptide (probability score: 0.953, cleavage site: amino acids 24-25)
219 (Supplementary Fig. 4a). Phylogenetic analysis demonstrated the high conservation of this novel
220 effector in aphid species, particularly in close relation to another cereal aphid, the corn leaf
221 aphid, *R. maidis* (Supplementary Fig. 4b).

222

223 **Disrupting diurnally rhythmic salivary effectors alters feeding dynamics and performance.**

224 We further determined the role of C002 and E8696 in aphid feeding and performance through
225 RNA interference. A significant knockdown of C002 and E8696 expression was confirmed at 24
226 hpi, with significant C002 silencing sustaining until 48 hpi (Fig. S2c-d). Silencing efficiencies at
227 24 and 48 hpi were 37% and 27% for C002 and 29% and 26% for E8696, respectively. Silencing
228 C002 reduced aphid survivorship and fecundity on wheat (Fig. 4e-f), consistent with previous
229 findings [24,26,44]. Specifically, C002 silencing caused 29% aphid mortality and a 56% reduction in
230 fecundity at 96 hpi compared to dsGFP control. Similarly, silencing of E8696 reduced aphid
231 survivorship and fecundity, causing a 79% mortality and 86% reduction in fecundity at 96 hpi.

To uncouple the influence of plant-derived cues on aphid feeding, we also assessed aphid performance on artificial diets after silencing the two effector genes. In contrast to the results observed on wheat plants, silencing either gene did not affect aphid survivorship and fecundity (Fig. 4g-h).

On plants, silencing either effector gene reduced overall honeydew excretion, with only C002 silencing disrupting the diurnal rhythm in honeydew excretion (Fig. 4i). Nighttime honeydew excretion decreased by 1.7- and 1.4-fold compared to the day after silencing C002 (4.1 vs 2.4) and E8696 (4.1 vs 2.9). In contrast, silencing had no impact on honeydew excretion on artificial diets, and aphids consistently generated more honeydew droplets at night than during the day (Fig. 4j). Furthermore, we found no diurnal variation in nymph production post-silencing on both plant and diet (Supplementary Fig. 5). However, the overall number of nymphs was markedly lower compared to dsGFP controls on the plant, but not on the diet. These findings emphasize the time-oriented roles of these effectors in aphid feeding on plants.

Disturbed aphid feeding activities were also confirmed using EPG after silencing E8696. Aphids exhibited an increase in the average duration (total duration/number of each event) of the salivation phase (E1), accompanied by a concurrent decrease in the phloem ingestion phase (E2) (Fig. 4k, Supplementary Data 5). These findings support our hypothesis that aphid feeding behavior and performance are tightly linked to and influenced by the diurnal expression of salivary effectors.

Discussion

The cyclical patterns of environmental cues, dictated by the earth's light-dark cycle, significantly influence the physiology and behavior of organisms, including crop plants and their pests [1,6]. While studies have begun to show the prevalence of diurnal rhythms among aphid pests, critical knowledge gaps persist regarding how these rhythms facilitate interactions between aphids and their hosts. Our study aimed to fill these knowledge gaps by exploring diurnal rhythms in behavior and gene expression in the bird-cherry oat aphid (*R. padi*), a major pest on cereals worldwide. We further characterized the impact of diurnally rhythmic osmoregulatory and salivary effector genes on *R. padi* behavior and performance.

Here, we found that aphids exhibited diurnal rhythms in feeding behaviors, particularly in honeydew excretion and the duration of phloem salivation (E1 phase). Contrary to previously documented patterns [10,11], *R. padi* excreted more honeydew droplets on wheat plants during the nighttime. This divergence in honeydew excretion patterns implies species-specific adaptations of aphids to host plants, possibly indicating differences in aphid osmoregulatory rhythms in response to phloem quality across host species. Notably, the diurnal honeydew excretion patterns persisted in *R. padi* on artificial diets, devoid of plant-derived cues, suggesting a potential internal circadian clock-driven mechanism. However, it should be noted that these experiments were only conducted in the absence of plant-derived cues. To determine the involvement of the circadian clock in regulating the rhythms uncovered in our study, all cues, including plant, light, and temperature, would need to be removed.

Remarkably, the pronounced nighttime increase in phloem salivation suggests that aphids may be responding to changes in plant defenses or phloem quality, both of which are known to exhibit diurnal variation in numerous plant species [45–47]. We also found that the duration of phloem and xylem sap ingestion (E2 and G phases, respectively) showed no significant differences over a 24 h cycle. The desire for aphids to quickly reach and remain in the E2 phase regardless of timepoint, coupled with the strong diurnal variation in honeydew excretion, might suggest that aphids do not modulate feeding behavior as a tool for osmoregulation but rather rely on metabolic mechanisms to process and excrete excess sugar. The low occurrence and the lack of diurnal variation in the G phase further suggests that increased metabolism of ingested phloem sap, resulting in higher honeydew excretion, constitute the primary mechanism for aphid osmoregulatory function over a 24 h period, with xylem ingestion only occurring in aphids that are severely dehydrated. These findings align with the nutritional and reproductive strategy of aphids, emphasizing the importance of acquiring sufficient sugar and amino acids for population growth and survival.

Our time-course profiling of aphid transcriptome revealed that approximately 9% of the total assembled transcripts displayed diurnal rhythms. Most rhythmic transcripts showed acrophases 6 h after the start and end of the light cue (noon or 4zt and midnight or 16zt, respectively). The bimodal pattern of these acrophases suggests that noon and midnight are periods of high activity in aphids, with multiple physiological and behavioral processes occurring at or around these times. Similar diurnal rhythmicity in gene expression was observed in Drosophila and the malaria mosquito (*Anopheles gambiae*), estimating rhythmic expression in 10% and 15.8% of genes linked to various biological functions [45–48], respectively. Clustered rhythmic transcripts, showing peak expressions at specific times of the day, point to a transcriptional control mechanism, possibly by the circadian clock. Our enrichment analysis highlights the functional diversity within the different rhythmic gene clusters, particularly in metabolic activities between the day and night. Notably, the night-peaking clusters 2 and 3 were enriched in pathways related to the metabolism of carbohydrates, amino acids, lipids, and other small molecules. The upregulation of these metabolic pathways at night corresponds with the observed diurnal rhythms in honeydew excretion, suggesting a correlation between these metabolic processes and the regulation of honeydew excretion.

Previous studies show that silencing AQP1 and SUC1 in *M. persicae* led to elevated hemolymph osmotic pressure, accompanied by a decrease in aphid weight and fecundity [32]. In our study, a parallel decline in aphid performance was observed, where the silencing of AQP1 and SUC1 in *R. padi* resulted in increased mortality and diminished fecundity. Notably, both genes exhibit a pronounced diurnal rhythm, suggesting their peak osmoregulatory activities at specific times of day, potentially linked to changes in phloem sap composition. An important aspect of osmoregulation in aphids is the excretion of excess sugar in the form of oligosaccharides in honeydew [27]. The overall reduction in quantity and the abolition of rhythms in honeydew excretion upon the silencing of AQP1 and SUC1 confirm their pivotal roles in shaping diurnal behavior of aphid honeydew excretion.

While we found that *R. padi* spent similar amounts of time feeding from the phloem cells during both day and night, a significant increase in salivation was observed at the beginning of the night. This suggests that time-of-day variations in the host plant may prompt aphids to modulate host responses through salivation and the introduction of specific effectors. Indeed, we found clear evidence showing diurnal rhythms in the expression of several salivary effector genes, including C002. The dynamic expression patterns of these rhythmic effectors suggest that different blends of effectors may be introduced into the plant for modulating time-of-day specific host plant responses.

To further confirm the time-dependent role of these rhythmic effectors in aphid-plant interactions, we silenced the C002 and E8696 effector genes, both showing peak expression at night. Silencing these two genes caused high mortality and reduced fecundity in aphids when feeding on host plants. However, no such trend was observed when the same experiment was performed on artificial diets, which underscores the crucial role of these effectors in facilitating the successful colonization of host plants by aphids. Strikingly, silencing these two effectors also resulted in a more pronounced reduction in nighttime honeydew excretion compared to the day on host plants. However, it had no impact on diurnal honeydew excretion on artificial diets. This affirms their significant roles in optimizing aphid feeding strategies and potentially enhancing their adaptation to the host plant's physiological changes during the night. Future research is warranted to elucidate whether the rhythmic activity of these effectors is driven by the aphid's circadian clock, phloem sap compositions, plant defenses, environmental changes across the diurnal period, or some combination of these factors.

In summary, our findings demonstrate significant alterations in the behavior and physiology of a major agricultural pest throughout the day. Exploring the daily variations in insect pests offers a new perspective for understanding the molecular, behavioral, and ecological factors that shape insect-plant interactions. Furthermore, the knowledge gained by these experiments holds great potential to inform the development of innovative pest control strategies. By strategically leveraging the daily rhythms that mark periods of strength and vulnerability in both crop plants and their pests, we envision entering an era of "chronoculture," [6] where harnessing circadian rhythms contributes significantly to enhancing crop yield and promoting sustainability.

Methods

Aphid colonies and plant growth conditions

A colony of bird cherry-oat aphids (*Rhopalosiphum padi*) was initiated with aphids collected from greenhouses at the Plant Growth Facility at Colorado State University, Fort Collins, and has been maintained in the laboratory since 2019. *R. padi* was reared on three-week-old barley seedlings (*Hordeum vulgare* var. AC Metcalfe). Colony plants were replenished every two to three weeks or when overcrowding occurred. All plants were grown in PRO-MIX BX General Purpose Growing Medium (Premier Tech Horticulture, Quakertown, PA) in mylar plant growth tents at 60-70% relative humidity, temperature of 24 ± 1ºC and maintained under a short-day

352 photoperiod of 12L:12D at photosynthetically active radiation (PAR) of 460 μmol/m^2/s. Plants
353 were watered three times per week and fertilized with Miracle Gro® (Scott's Co. LLC,
354 Marysville, OH, USA) once a week. All experiments were performed on wheat (*Triticum*
355 *aestivum* var. Chinese Spring) plants that were 14-21 days old or at the two-leaf stage (Zadoks
356 stage, Z1.2) [48].

357 **Aphid age synchronization**

358 All experiments used age-synchronized aphids to limit any age-related effects on aphid behaviors
359 or gene expression [49]. Briefly, adult aphids from the colony were placed into a feeding chamber
360 containing the second and third leaves of a two-week-old wheat plant. The feeding chamber was
361 made from a 50-ml falcon tube with the bottom side cut open and the lid modified for ventilation
362 using aphid-proof mesh. Leaves were inserted into the tube from the bottom opening and sealed
363 with a cotton ball. After 48 h, adult aphids were removed, and nymphs were allowed to develop
364 to adulthood on the plant for five days.

365 **Aphid feeding assay on wheat and artificial diet**

366 Five age-synchronized aphids were placed into a 55 mm Petri dish (V.W.R., Radnor, PA)
367 modified to contain leaf 2 of a wheat plant (Z1.2) (Fig. 5a). Nymph count and honeydew droplet
368 production were recorded at the onset of day and night over 48 h, adhering to a 12L:12D
369 photoperiod. Discrete honeydew droplets were counted instead of using a staining and area
370 calculation method. This choice was made because droplets exhibit uniform size and were easily
371 visible to the naked eye. However, their translucent color made capturing them in photographs
372 and measuring the area challenging. After each measurement, nymphs were carefully removed,
373 and the honeydew-soiled lid was replaced with a fresh one. Concurrently, feeding assays were
374 conducted using an artificial diet designed for *R. padi* [50]. An artificial feeding chamber was
375 constructed under sterile conditions and consisted of 58 mm Petri-dish lids with Parafilm sachets
376 containing 1.5 ml of diet. Five age-synchronized aphids were placed into the artificial feeding
377 chamber (Fig. 5a) and the number of nymphs and honeydew droplets were measured as
378 described above. Both experiments were independently conducted on two occasions, with five
379 replicates on each occasion (n = 10 for each experiment on wheat or diet). Statistical differences
380 between treatments were tested using the Mann-Whitney test ($P < 0.05$) in Graphpad Prism v10.

381 **Electrical penetration graph**

382 Adult *R. padi* feeding behavior was recorded on wheat seedlings (Z1.2) using the electrical
383 penetration graph (EPG) [51] technique on a GIGA 8 complete system (EPG systems, Wageningen,
384 Netherlands). The recordings were performed every 4 h over a 24 h period starting at 0zt (a total
385 of six time periods). Age-synchronized adult *R. padi* were starved for 1 h before wiring. Next,
386 plant electrodes were inserted into the soil, and insect probes were adjusted to ensure contact
387 between the plant surface and the insect. Aphids were only allowed to feed from the leaf 2, and
388 only one aphid was recorded per plant. For recordings that were initiated in the night or
389 scotophase (0zt, 16zt, and 20zt), all setup was performed with a red LED headlight (Energizer).
390 The 0zt timepoint was set up in dark conditions while feeding behavior was recorded in light.
391 The 12zt timepoint was set up in light conditions, with feeding behavior recorded in darkness.

392 Photoperiod and the temperatures during the day and night were the same as those used for plant
393 and aphid growing conditions. Both plants and aphids were discarded after each 4 h recording.
394 EPG waveforms were analyzed using the Stylet+ software (v01.25, EPG systems, Wageningen,
395 the Netherlands). The analysis of each feeding experiment aimed to determine the time allocation
396 across four primary phases: the pathway or probing phase (C), non-probing phase (NP),
397 salivation phase (E1), phloem sap ingestion phase (E2), and xylem phase (G). Additionally,
398 many EPG parameters that characterize aphid probing and ingestion [52] were determined to
399 develop a comprehensive picture of aphid feeding over a 24 h period. EPG parameters were
400 calculated using the discoEPG package integrated into the web-based R/shiny app
401 (https://nalamlab.shinyapps.io/test/). The source code used for discoEPG software development
402 is available on GitHub platform (https://github.com/nalamvj/EPG_ANALYSIS). There were 25
403 replicates for 0zt, 21 replicates for 4zt, 26 replicates for 8zt, 23 replicates for 12zt, 29 replicates
404 for 16zt, and 16 replicates for 20zt. Recordings without feeding or probing events and those with
405 more than 70% of time spent in NP + derailed stylet phase (F) + G were excluded from the
406 analysis. Statistical differences between the six time periods of each EPG phase were tested
407 using the Kruskal–Wallis test with Bonferroni adjustment for *p*-values (adjusted $P < 0.05$). The
408 rhythmicity of EPG phases was determined with the average total duration (minutes) of each
409 recorded waveform across the different periods using a Cosinor-based oscillation detection
410 method in DiscoRhythm v1.2.1 [53]. EPG phases were considered significant rhythmic if their *p*-
411 values were less than 0.05, and their corresponding oscillation parameters were estimated.

412 **Sample collection, RNA isolation, library preparation, and RNA Sequencing**

413 A cohort of adult *R. padi* (~100) were evenly distributed on wheat plants (Z1.2). The adults were
414 removed after 24 h, and the nymphs were allowed to develop to adulthood for six days. These
415 age-synchronized *R. padi* adults were collected from wheat plants every four hours over a 24 h
416 period (12L:12D), starting at 0zt (when the lights were turned on) and ending at 20zt (Fig. 5b). A
417 pool of 30 apterous aphids was collected per sample and extracted for total RNA using the
418 Quick-RNA Miniprep Kit (Zymo Research, Irvine, CA) according to the manufacturer's
419 instructions. This time-course RNA-Seq experiment comprised three biological replicates of
420 aphid samples per time point. RNA quality and concentration were measured using a Nanodrop
421 spectrophotometer (Thermo Scientific, Waltham, MA) and Agilent 2100 Bioanalyzer (Santa
422 Clara, CA). Aphid RNA samples were sent to Novogene Corporation Inc. (Sacramento, CA) for
423 cDNA library construction and RNA sequencing. The poly(A) mRNA-enriched libraries were
424 constructed using NEBNext® Ultra™ II RNA Library Prep Kit (New England BioLabs, Ipswich,
425 MA). Paired-end sequencing (2×150 bp) was conducted with the Illumina HiSeq 2000 platform.
426 The raw sequencing reads have been deposited in the NCBI SRA database under the BioProject
427 accession PRJNA979927.

428 **Genome-guided transcriptome assembly and read mapping**

429 Raw sequence reads were trimmed for adapters and quality using fastp v0.23.3[54]. The reads with
430 a Phred score less than 25 and lengths shorter than 100 bp were discarded. The high-quality reads
431 from each library were mapped against the *R. padi* reference genome (v2.0) available on
432 AphidBase (https://bipaa.genouest.org/is/aphidbase/) using Hisat2 v2.2.1. The mapped reads

were assembled into transcripts using Stringtie v2.2.1. The assemblies from all 18 libraries were further merged to generate a reference transcriptome using the Stringtie -merge function [55]. Reads representing each sampling timepoint were mapped back to this reference transcriptome to quantify the gene expression using Salmon v1.9.0 [56].

Identification and clustering of diurnal rhythmic transcripts

The non-random rhythmicity of *R. padi* genes was determined with a Cosinor-based oscillation detection method in DiscoRhythm v1.2.1 [53]. The temporal expression data of all transcripts identified in the whole-body *R. padi* (48,690) were utilized for detecting rhythmic signals. The expression data was filtered for constant or missing values (>25%) across the samples, resulting in 38,871 transcripts. Rhythm detection and estimation of oscillation parameters were performed as previously outlined. Soft clustering of all rhythmic sequences was carried out to identify major temporal patterns of rhythmic expression using the R package, mFuzz v2.56.0 [43]. Membership values ranging from 0 to 1 were assigned to clustered transcripts. Sequences with a membership value > 0.7 were considered core members of each cluster [57].

Gene ontology and pathway enrichment analyses

All clustered sequences of rhythmic transcripts in *R. padi* were blastx-searched against the NCBI non-redundant (nr) protein database using OmicsBox v2.2 with an E-value cut-off of 1e-5 [58]. Sequences with assigned gene ontology (GO) terms were categorized into biological process, molecular function, and cellular component categories. Further, these clustered sequences were annotated for the Kyoto Encyclopedia of Genes and Genomes (KEGG) orthologs and linked to corresponding KEGG reference pathways. GO and KEGG pathway enrichment analyses were performed for rhythmic transcripts within each of the four gene clusters and the rhythmic putative salivary effector transcripts using a two-tailed Fisher's exact test with an FDR cut-off of 0.05 in OmicsBox [58]. The entire *R. padi* transcriptome was used as the background gene set for both enrichment analyses.

Identification of diurnally rhythmic osmoregulatory and putative salivary effector genes

Osmoregulatory genes in *R. padi* were identified as described previously [16]. Briefly, homologs for these genes were identified by querying *Acyrthosiphon pisum* gene sequences with the *R. padi* reference genome (v2.0) on AphidBase [59] using Blastp. Further validation involved searching protein sequences with DeepTMHMM [60] and SMART [61] to determine the presence of sequence features. All *R. padi* transcripts were searched against the curated putative salivary effector database for *R. padi* [23] using Blast+ v2.13.0 with an E-value cut-off of 1e-5. Stringent criteria were applied, with thresholds set at 80% for identity and 50% for coverage to identify putative salivary effectors. To quantify tissue-specific expression of these rhythmic putative effectors, RNA-Seq reads of *R. padi* heads and bodies (not including heads and nymphs) were retrieved through the European Nucleotide Archive under the project accession number of PRJEB9912 [23]. Sample accessions for head and body datasets are as follows: SAMEA3505144, SAMEA3505145, SAMEA3505146, SAMEA3505147, SAMEA3505148, SAMEA3505149. Reads were trimmed for adapters and quality and mapped against the previously assembled *R. padi* reference transcriptome using the abovementioned pipeline. The diurnal rhythmicity of

473 identified osmoregulatory and putative effector sequences was tested using the Cosinor model
474 described above.

475 **Sequence and phylogenetic analyses of a novel putative salivary effector**

476 The full-length coding sequence of E8696 was queried against the NCBI nr protein database with
477 organism specified as aphids. There were 25 sequence hits in the database for E8696. The top hit
478 of each aphid species was retrieved and used for sequence analysis (Supplementary Table 5).
479 Signal peptide, transmembrane helix, and other conserved domains were analyzed using SignalP
480 v6.0, DeepTMHMM, and NCBI Conserved Domain Search [62–64]. Multiple sequence alignments
481 were performed using MUSCLE, and the phylogenetic trees were built using the maximum
482 likelihood method with GTR+G as the best-fit substitution model in MEGA 11 software [65]. Node
483 support rates were assessed with 1,000 bootstrap replicates.

484 **Design and synthesis of double-stranded RNAs**

485 Sequence analysis was performed on the four target genes: AQP1, SUC1, C002, and E8696. The
486 open reading frames and potential conserved domains were identified using the NCBI ORFfinder
487 and Conserved Domain Search tools [64]. The nucleotide sequence of each gene was evaluated to
488 identify optimal target regions of double-stranded RNA (dsRNA). Corresponding primers were
489 designed using the E-RNAi web tool [66] (Supplementary Table 6). The specificity of dsRNA
490 primers was confirmed through a search against the NCBI *R. padi* nr database using the Primer-
491 BLAST tool and in PCR, followed by agarose gel electrophoresis. For dsRNA synthesis, total
492 RNA was extracted from a pool of ~30 *R. padi* containing all five developmental stages using
493 Direct-zol RNA Microprep Kit (Zymo Research, Irvine, CA) according to the manufacturer's
494 protocol. cDNA was synthesized from 1 µg of DNase-treated RNA using the Verso cDNA
495 Synthesis Kit (Thermo Scientific, Waltham, MA). The dsRNA sequence region of each gene was
496 amplified with the gene-specific primer pair using Q5 high-fidelity PCR (New England BioLabs,
497 Ipswich, MA). The sense and antisense dsRNA sequence fragments conjugated with the T7
498 promoter sequence were amplified separately using the previous PCR amplicons as templates.
499 All PCR products were confirmed for unique and accurate amplification in agarose gels and
500 purified using GeneJET PCR Purification Kit (Thermo Scientific, Waltham, MA). dsRNA was
501 synthesized with 1 µg of purified PCR products using the T7 RiboMAX Express RNAi System,
502 according to the manufacturer's instructions (Promega, Madison, WI). dsRNA targeting the green
503 fluorescent protein (GFP) gene was synthesized following the protocol described above and used
504 as a negative control. The quantity and integrity of dsRNA were measured by Nanodrop
505 spectrophotometer (Thermo Scientific, Waltham, MA) and agarose gel electrophoresis.

506 **Microinjection of aphids with dsRNA**

507 Injection needles (Drummond Scientific Co., Broomall, PA) were produced by pulling with a P-
508 1000 micropipette puller (Sutter Instrument Co. Novato, CA) using optimized settings:
509 heat=500, pull=100, velocity=40, delay=100, pressure=500, and ramp=493. The glass needle,
510 filled with 5 µl of dsRNA, was assembled onto a Nanoject III microinjector (Drummond
511 Scientific Co., Broomall, PA). Age-synchronized aphids were immobilized on a sticky tape strip
512 (ventral side up) and injected with 180 ng of dsRNA (40 nl of 4.5 µg/µl) through the flexible

513 membrane between the coxa of the hind leg and thorax. Immediately after injection, aphids were
514 carefully detached from the tape using a wet paintbrush and transferred to a feeding chamber
515 containing wheat leaves. The injection process was repeated until the desired number of aphids
516 was achieved. The same procedure was applied to the other dsRNA treatment groups. The
517 injected aphids were incubated at 25°C, 12L:12D photoperiod. Each experiment was
518 independently replicated three times.

519 **Gene silencing in aphids**

520 Five aphids, collected at 24- and 48-hour post-injection from three biological replicates, were
521 subjected to RNA extraction using the Direct-zol® RNA Microprep Kit as described above.
522 cDNA was synthesized from 500 ng of RNA and diluted 4-fold with nuclease-free water.
523 Quantitative PCR (qPCR) was employed to measure the expression of the target gene and the
524 housekeeping gene, Actin (AphidBase accession - g9633.t1). Gene-specific qPCR primers were
525 designed using the NCBI Primer-Blast tool (Supplementary Table 6). A duplicate of 10 µl SYBR
526 Green Supermix reaction (Bio-Rad, Hercules, CA) containing 2 µl of cDNA template was
527 prepared and analyzed using CFX Connect Real-Time instrument (BioRad) with the following
528 thermocycling conditions: 95°C for 30s, followed by 40 cycles of 95°C for 10s, 55°C for 30s,
529 72°C for 30s, with a final melt curve of 95°C for 30s, 65°C for 5s increasing to a final
530 temperature of 95°C. The relative normalized expression of each target gene was estimated using
531 the Pfaffl method [67]. Statistical differences in gene expression between treatments at each time
532 point were assessed using a two-tailed Welch's *t*-test ($P < 0.05$) in Graphpad Prism v10.

533 **Aphid performance and feeding assays on wheat and artificial diet after gene knockdown**

534 RNA interference (RNAi) was used to functionally characterize two osmoregulatory genes,
535 aquaporin 1 (AQP1) and gut sucrase 1 (SUC1). Nine aphids injected with dsRNA AQP1
536 (dsAQP1) or dsRNA SUC1 (dsSUC1) were placed into a feeding chamber containing wheat
537 leaves (Fig. 5a). Aphid mortality and fecundity (cumulative nymph count) were recorded every
538 24 h for 4 days. Aphids injected with dsRNA GFP (dsGFP) were the negative control. The
539 number of honeydew droplets produced by five dsRNA-injected aphids on wheat plants were
540 recorded at the beginning of the day and night for 4 days under a short-day photoperiod as
541 described previously (Fig. 5a). Similar experimental setups were replicated for two target
542 salivary effector genes, C002 and E8696, to measure aphid mortality and fecundity. Additionally,
543 five aphids injected with dsRNA C002 (dsC002) or dsRNA E8696 (dsE8696) were placed on an
544 artificial diet (Fig. 5b) and monitored for mortality and fecundity every 24 h for 4 days. To
545 further assess daily changes in honeydew excretion and fecundity, five aphids after 24 h post-
546 injection with dsC002 or dsE8696 were placed on a wheat leaf or artificial diet. The numbers of
547 honeydew droplets and nymphs were recorded as previously described (Fig. 5a). All experiments
548 were independently repeated three times. Kaplan-Meier survival curves were generated for
549 dsRNA-injected aphids and compared for statistical differences by the Mantel-Cox log-rank test
550 with Benjamini–Hochberg false discovery rate adjusted *p*-values (adjusted $P < 0.05$) using the
551 Survminer v0.4.9. The statistical difference in the nymph count of dsRNA-injected aphids was
552 determined using a repeated measures ANOVA test with Tukey's multiple comparisons (adjusted
553 $P < 0.05$). The normality of input data was confirmed using the Shapiro-Wilk test ($P > 0.05$).

Statistical differences in honeydew and nymph productions between treatments were tested using the Mann-Whitney test ($P < 0.05$) and Kruskal-Wallis test, followed by Dunn's multiple comparison tests (adjusted $P < 0.05$). The statistical analyses were performed using Graphpad Prism v10 and R v4.2.1.

Electrical penetration graph after silencing E8696

Age-synchronized *R. padi* were injected with dsE8696 or dsGFP as described above. Twenty-four hours post microinjection, individual aphids were wired and subjected to EPG recording to document their feeding activities on wheat plants (Z1.2) as described previously. Recordings started at 0zt, and feeding behavior was recorded for 8 h for each aphid. The experiment included 13 replicates for dsE8696 and 15 replicates for the dsGFP control group. EPG parameters were calculated as previously described, and statistical differences between the two treatments were tested using the Mann-Whitney test ($P < 0.05$).

Statistical analysis

The statistical tests employed for assessing significance between treatments were described in the respective sections above. All statistical analyses were performed in Graphpad Prism v10 and R v4.2.1.

Data availability

The raw RNA sequencing reads of *Rhopalosiphum padi* have been deposited under the BioProject accession number PRJNA979927 in the Sequence Read Archive (SRA). Reference genome of *R. padi* (v2.0) can be found in AphidBase (https://bipaa.genouest.org/is/). All other data supporting the findings of this study are available in the article, Supplementary Information files, Source Data file, or from the corresponding author upon request. Source data are provided with this paper.

Code availability

All code and software sources used in this study are described in the “Methods” section with corresponding citations of references, links to source codes, and Source Data file.

Acknowledgments

We thank Joely Corrales for her assistance with planting and aphid synchronization. Drs. Jan Leach, Micky Eubanks, and Punya Nachappa for internal review of the manuscript. The project was funded by the United States – Israel Binational Science Foundation grant (Proposal#202181, PIs Vered Tzin and Vamsi Nalam), Research Capacity Fund (COL0044) from NIFA and start-up funds from Colorado State University to Vamsi Nalam.

Author Contributions: J.H., D.K., V.T, and V.J.N designed the research; J.H., D.K., Y.G., and M.C. performed the research; J.H., D.K., M.C., Y.G., V.T, and V.J.N analyzed the data; and J.H., D.K., V.T, and V.J.N wrote the paper.

Competing Interests: The authors declare no competing interests.

References

1. Bhadra, U., Thakkar, N., Das, P. & Pal Bhadra, M. Evolution of circadian rhythms: from bacteria to human. *Sleep Med* **35**, 49–61 (2017).

2. Vitaterna, M. H., Takahashi, J. S. & Turek, F. W. Overview of Circadian Rhythms. *Alcohol Research & Health* **25**, 85 (2001).

3. Beer, K. & Helfrich-Förster, C. Model and Non-model Insects in Chronobiology. *Front Behav Neurosci* **14**, 221 (2020).

4. Rund, S. S. C., O'Donnell, A. J., Gentile, J. E. & Reece, S. E. Daily rhythms in mosquitoes and their consequences for malaria transmission. *Insects* vol. 7 Preprint at https://doi.org/10.3390/insects7020014 (2016).

5. Hotta, C. T. From crops to shops: How agriculture can use circadian clocks. *Journal of Experimental Botany* vol. 72 Preprint at https://doi.org/10.1093/jxb/erab371 (2021).

6. Steed, G., Ramirez, D. C., Hannah, M. A. & Webb, A. A. R. Chronoculture, harnessing the circadian clock to improve crop yield and sustainability. *Science (1979)* **372**, (2021).

7. Dedryver, C. A., le Ralec, A. & Fabre, F. The conflicting relationships between aphids and men: A review of aphid damage and control strategies. *C R Biol* **333**, 539–553 (2010).

8. Goodspeed, D., Chehab, E. W., Min-Venditti, A., Braam, J. & Covington, M. F. Arabidopsis synchronizes jasmonate-mediated defense with insect circadian behavior. *Proc Natl Acad Sci U S A* **109**, 4674–4677 (2012).

9. Liu, J. *et al.* Spider Mites Cause More Damage to Tomato in the Dark When Induced Defenses Are Lower. *J Chem Ecol* **46**, (2020).

10. Lei, J. *et al.* CIRCADIAN CLOCK-ASSOCIATED1 controls resistance to aphids by altering indole glucosinolate production. *Plant Physiol* **181**, 1344–1359 (2019).

11. Beer, K., Joschinski, J., Arrazola Sastre, A., Krauss, J. & Helfrich-Förster, C. A damping circadian clock drives weak oscillations in metabolism and locomotor activity of aphids (Acyrthosiphon pisum). *Scientific Reports 2017 7:1* **7**, 1–9 (2017).

12. Eisenbach, J. & Mittler, T. E. An aphid circadian rhythm: Factors affecting the release of sex pheromone by oviparae of the greenbug, Schizaphis graminum. *J Insect Physiol* **26**, 511–515 (1980).

13. Hodgson, C. J. & Lane, I. R. Some effects of photoperiod on larviposition and fresh weight-gain in Myzus persicae. *Physiol Entomol* **6**, (1981).

14. Joschinski, J., Beer, K., Helfrich-Förster, C. & Krauss, J. Pea aphids (Hemiptera: Aphididae) have diurnal rhythms when raised independently of a host plant. *Journal of Insect Science* **16**, (2016).

629 15. Matsuda, N. Hatching rhythm and clock gene expression in the egg of the pea aphid,
630 Acyrthosiphon pisum. *J Insect Physiol* **145**, (2023).

631 16. Nalam, V. *et al.* Diurnal feeding as a potential mechanism of osmoregulation in aphids.
632 *Insect Sci* **28**, 521–532 (2021).

633 17. Douglas, A. E. The Nutritional Physiology of Aphids. *Advances in Insect Physiology* vol.
634 31 Preprint at https://doi.org/10.1016/S0065-2806(03)31002-1 (2003).

635 18. Douglas, A. E. Phloem-sap feeding by animals: Problems and solutions. in *Journal of*
636 *Experimental Botany* vol. 57 (2006).

637 19. van Bel, A. J. E. & Will, T. Functional evaluation of proteins in watery and gel saliva of
638 aphids. *Front Plant Sci* **7**, 1840 (2016).

639 20. Mondal, H. A. Aphid saliva: a powerful recipe for modulating host resistance towards
640 aphid clonal propagation. *Arthropod Plant Interact* **14**, 547–558 (2020).

641 21. Bos, J. I. B. *et al.* A functional genomics approach identifies candidate effectors from the
642 aphid species Myzus persicae (green peach aphid). *PLoS Genet* **6**, (2010).

643 22. Carolan, J. C. *et al.* Predicted effector molecules in the salivary secretome of the pea aphid
644 (Acyrthosiphon pisum): A dual transcriptomic/proteomic approach. *J Proteome Res* **10**,
645 1505–1518 (2011).

646 23. Thorpe, P., Cock, P. J. A. & Bos, J. Comparative transcriptomics and proteomics of three
647 different aphid species identifies core and diverse effector sets. *BMC Genomics* **17**,
648 (2016).

649 24. Mutti, N. S. *et al.* A protein from the salivary glands of the pea aphid, Acyrthosiphon
650 pisum, is essential in feeding on a host plant. *Proc Natl Acad Sci U S A* **105**, 9965 (2008).

651 25. Mutti, N. S., Park, Y., Reese, J. C. & Reeck, G. R. RNAi knockdown of a salivary
652 transcript leading to lethality in the pea aphid, Acyrthosiphon pisum. *Journal of Insect*
653 *Science* **6**, (2006).

654 26. Pitino, M., Coleman, A. D., Maffei, M. E., Ridout, C. J. & Hogenhout, S. A. Silencing of
655 aphid genes by dsRNA feeding from plants. *PLoS One* **6**, (2011).

656 27. Wilkinson, T. L., Ashford, D. A., Pritchard, J. & Douglas, A. E. Honeydew Sugars and
657 Osmoregulation in the Pea Aphid Acyrthosiphon Pisum. *Journal of Experimental Biology*
658 **200**, 2137–2143 (1997).

659 28. Fisher, D. B., Wright, J. P. & Mittler, T. E. Osmoregulation by the aphid Myzus persicae:
660 A physiological role for honeydew oligosaccharides. *J Insect Physiol* **30**, (1984).

661 29. Spiller, N. J., Koenders, L. & Tjallingii, W. F. Xylem ingestion by aphids – a strategy for
662 maintaining water balance. *Entomol Exp Appl* **55**, (1990).

30. Karley, A. J., Ashford, D. A., Minto, L. M., Pritchard, J. & Douglas, A. E. The significance of gut sucrase activity for osmoregulation in the pea aphid, Acyrthosiphon pisum. *J Insect Physiol* **51**, 1313–1319 (2005).

31. Shakesby, A. J. *et al.* A water-specific aquaporin involved in aphid osmoregulation. *Insect Biochem Mol Biol* **39**, 1–10 (2009).

32. Tzin, V. *et al.* RNA interference against gut osmoregulatory genes in phloem-feeding insects. *J Insect Physiol* **79**, (2015).

33. Cull, D. C. & Emden, H. F. V. The effect on Aphis fabae of diel changes in their food quality. *Physiol Entomol* **2**, (1977).

34. Gattolin, S. *et al.* A diurnal component to the variation in sieve tube amino acid content in wheat. *Plant Physiol* **147**, (2008).

35. Gomez, S. K., Oosterhuis, D. M., Hendrix, D. L., Johnson, D. R. & Steinkraus, D. C. Diurnal pattern of aphid feeding and its effect on cotton leaf physiology. *Environ Exp Bot* **55**, (2006).

36. Kallarackal, J., Bauer, S. N., Nowak, H., Hajirezaei, M. R. & Komor, E. Diurnal changes in assimilate concentrations and fluxes in the phloem of castor bean (Ricinus communis L.) and tansy (Tanacetum vulgare L.). *Planta* **236**, (2012).

37. Finlay, K. J. & Luck, J. E. Response of the bird cherry-oat aphid (Rhopalosiphum padi) to climate change in relation to its pest status, vectoring potential and function in a crop–vector–virus pathosystem. *Agric Ecosyst Environ* **144**, 405–421 (2011).

38. Cristofoletti, P. T., Ribeiro, A. F., Deraison, C., Rahbé, Y. & Terra, W. R. Midgut adaptation and digestive enzyme distribution in a phloem feeding insect, the pea aphid Acyrthosiphon pisum. *J Insect Physiol* **49**, 11–24 (2003).

39. Price, D. R. G. *et al.* Molecular characterisation of a candidate gut sucrase in the pea aphid, Acyrthosiphon pisum. *Insect Biochem Mol Biol* **37**, 307–317 (2007).

40. Price, D. R. G. & Gatehouse, J. A. Genome-wide annotation and functional identification of aphid GLUT-like sugar transporters. *BMC Genomics* **15**, (2014).

41. Toruño, T. Y., Stergiopoulos, I. & Coaker, G. Plant-Pathogen Effectors: Cellular Probes Interfering with Plant Defenses in Spatial and Temporal Manners. *Annual Review of Phytopathology* vol. 54 Preprint at https://doi.org/10.1146/annurev-phyto-080615-100204 (2016).

42. Yates-Stewart, A. D. *et al.* Soybean aphids adapted to host-plant resistance by down regulating putative effectors and up regulating transposable elements. *Insect Biochem Mol Biol* **121**, (2020).

43. Kumar, L. & Futschik, M. E. Mfuzz: A software package for soft clustering of microarray data. *Bioinformation* **2**, (2007).

699 44. Escudero-Martinez, C. *et al.* An aphid effector promotes barley susceptibility through
700 suppression of defence gene expression. *J Exp Bot* **71**, 2796 (2020).

701 45. Goodspeed, D., Chehab, E. W., Min-Venditti, A., Braam, J. & Covington, M. F.
702 Arabidopsis synchronizes jasmonate-mediated defense with insect circadian behavior.
703 *Proc Natl Acad Sci U S A* **109**, 4674–4677 (2012).

704 46. Winter, H., Lohaus, G. & Heldt, H. W. Phloem Transport of Amino Acids in Relation to
705 their Cytosolic Levels in Barley Leaves. *Plant Physiol* **99**, 996 (1992).

706 47. Gattolin, S. *et al.* A Diurnal Component to the Variation in Sieve Tube Amino Acid
707 Content in Wheat. *Plant Physiol* **147**, 912 (2008).

708 48. Zadoks, J. C., Chang, T. T. & Konzak, C. F. A decimal code for the growth stages of
709 cereals. *Weed Res* **14**, (1974).

710 49. Li, Y., Hill, C. B. & Hartman, G. L. Effect of three resistant soybean genotypes on the
711 fecundity, mortality, and maturation of soybean aphid (Homoptera: Aphididae). *J Econ*
712 *Entomol* **97**, (2004).

713 50. Auclair, J. L. Feeding and Nutrition of the Pea Aphid, Acyrthosiphon pisum (Homoptera:
714 Aphidae), on Chemically Defined Diets of Various pH and Nutrient Levels1. *Ann Entomol*
715 *Soc Am* **58**, 855–875 (1965).

716 51. Tjallingii, W. F. & Esch, T. H. Fine structure of aphid stylet routes in plant tissues in
717 correlation with EPG signals. *Physiol Entomol* **18**, (1993).

718 52. Sarria, E., Cid, M., Garzo, E. & Fereres, A. Excel Workbook for automatic parameter
719 calculation of EPG data. *Comput Electron Agric* **67**, 35–42 (2009).

720 53. Carlucci, M. *et al.* DiscoRhythm: An easy-to-use web application and R package for
721 discovering rhythmicity. *Bioinformatics* **36**, (2020).

722 54. Chen, S., Zhou, Y., Chen, Y. & Gu, J. Fastp: An ultra-fast all-in-one FASTQ preprocessor.
723 in *Bioinformatics* vol. 34 (2018).

724 55. Pertea, M., Kim, D., Pertea, G. M., Leek, J. T. & Salzberg, S. L. Transcript-level
725 expression analysis of RNA-seq experiments with HISAT, StringTie and Ballgown.
726 *Nature Protocols 2016 11:9* **11**, 1650–1667 (2016).

727 56. Patro, R., Duggal, G., Love, M. I., Irizarry, R. A. & Kingsford, C. Salmon provides fast
728 and bias-aware quantification of transcript expression. *Nature Methods 2017 14:4* **14**,
729 417–419 (2017).

730 57. Futschik, M. E. & Carlisle, B. Noise-robust soft clustering of gene expression time-course
731 data. *J Bioinform Comput Biol* **3**, (2005).

732 58. Götz, S. *et al.* High-throughput functional annotation and data mining with the Blast2GO
733 suite. *Nucleic Acids Res* **36**, (2008).

734 59. Gauthier, J. P., Legeai, F., Zasadzinski, A., Rispe, C. & Tagu, D. AphidBase: A database
735 for aphid genomic resources. *Bioinformatics* **23**, (2007).

736 60. Hallgren, J. *et al.* DeepTMHMM predicts alpha and beta transmembrane proteins using
737 deep neural networks. *bioRxiv* (2022).

738 61. Letunic, I., Khedkar, S. & Bork, P. SMART: Recent updates, new developments and status
739 in 2020. *Nucleic Acids Res* **49**, (2021).

740 62. Teufel, F. *et al.* SignalP 6.0 predicts all five types of signal peptides using protein
741 language models. *Nat Biotechnol* **40**, (2022).

742 63. Høie, M. H. *et al.* NetSurfP-3.0: accurate and fast prediction of protein structural features
743 by protein language models and deep learning. *Nucleic Acids Res* **50**, (2022).

744 64. Lu, S. *et al.* CDD/SPARCLE: The conserved domain database in 2020. *Nucleic Acids Res*
745 **48**, (2020).

746 65. Tamura, K., Stecher, G. & Kumar, S. MEGA11: Molecular Evolutionary Genetics
747 Analysis Version 11. *Mol Biol Evol* **38**, (2021).

748 66. Horn, T. & Boutros, M. E-RNAi: A web application for the multi-species design of RNAi
749 reagents-2010 update. *Nucleic Acids Res* **38**, (2010).

750 67. Pfaffl, M. W. A new mathematical model for relative quantification in real-time RT–PCR.
751 *Nucleic Acids Res* **29**, (2001).

752

Figure Legends

Figure 1. Diurnal rhythmicity of aphid feeding behaviors. a, b The number of honeydew droplets produced by aphids was measured at the end of each 12h day and night cycle for 48h. Average number (±SE) of honeydew droplets produced per aphid on wheat plants (**a**, n=10) and artificial diet (**b**, n=10). Significant differences between day and night were tested by the two-tailed Mann-Whitney test (wheat: ***p=0.0006 and diet: *p=0.0411). **c, d** Aphid feeding activity was monitored every 4h over a 24h period, 0zt (n=25), 4zt (n=21), 8zt (n=26), 12zt (n=23), 16zt (n=29), and 20zt (n=16). The total time (±SE) spent by aphids in phloem salivation (E1) and phloem ingestion (E2) are shown in (**c**) and (**d**), respectively. Solid lines, boundaries, and whiskers indicate the median, 25th, and 75th percentiles and 1.5 interquartile ranges, respectively. Points indicate outliers. Different letters above the boxes denote significant differences (Kruskal-Wallis test followed by Dunn's multiple comparisons adjusted by Bonferroni for p-values, adj. p<0.05). Diurnal rhythmicity of E1 (**c**) and E2 (**d**) waveforms over 24h was assessed with Cosinor model. The curve line and shaded area represent the fitted periodic sinusoidal curve and 95% confidence band, respectively. Significance is only established for a diurnal rhythm if the Cosinor p-value is <0.05 (E1: p=0.0119 and E2: p=0.7313). Yellow and black bars at the x-axis mirror the day and night. ZT = Zeitgeber time. Source data and full statistical summary are provided in the Source Data file.

Figure 2. Diurnal rhythmicity of gene expression in *R. padi* and their roles in aphid feeding. a Acrophase frequency of diurnally rhythmic transcripts in *R. padi*. Each bar represents the number of rhythmic sequences with acrophase values in each 24h period. Numbers around the outer sphere indicate zeitgeber time (ZT). **b** Soft-clustering of diurnally rhythmic transcripts. High, medium, and low membership scores are color-coded with red, yellow, and blue lines. **c** Top-10 enriched KEGG pathways for diurnally rhythmic transcripts in each cluster. Circle size and color represent enriched gene number in a pathway and Benjamini-Hochberg adjusted p-value, respectively. Gene ratio indicates the percentage of diurnally rhythmic transcripts of a cluster. **d, e** Expression profile of two diurnally rhythmic osmoregulatory genes, aquaporin 1 (AQP1, **d**) and gut sucrase 1 (SUC1, **e**). Solid lines, boundaries, and whiskers of each box indicate median, 25th, and 75th percentiles and 1.5 interquartile ranges. Diurnal rhythmicity of AQP1 (p=0.031) and SUC1 (p=0.013) was determined with Cosinor model. The curve line and shaded area represent the fitted periodic sinusoidal curve and 95% confidence band, respectively. **f** Kaplan-Meier survival curves and **g** fecundities of aphids after treatment with dsRNA AQP1 (dsAQP1, n=3), dsRNA SUC1 (dsSUC1, n=3), and dsRNA GFP (dsGFP, n=3, negative control). Significant differences in survivorship and fecundity were tested using a log-rank test with Benjamini-Hochberg adjustment (dsAQP1 vs dsGFP: *p=0.0272 and dsSUC1 vs dsGFP: ***p=0.0003) and a repeated measures ANOVA with Dunn's multiple comparisons test (*p<0.05, **p<0.01, ***p<0.001, ****p<0.0001), respectively. **h** Average number (±SE) of honeydew droplets produced per aphid after treatment with dsAQP1 (n=5), dsSUC1 (n=3), and dsGFP (n=5) on wheat. Yellow and black bars represent the average number of droplets produced at the end of each 12:12h day and night for 4 days (Mann-Whitney test, **p<0.01, ****p<0.0001, NS=no significant difference). Source data and full statistical summary are provided in the Source Data file.

Figure 3. Diurnally rhythmic putative salivary effectors in *R. padi*. a Heatmap showing temporal gene expression patterns of 42 diurnally rhythmic putative salivary effectors. Each row and column represents the salivary effectors and zeitgeber time (ZT). The hierarchical clustering of gene expression data was generated using one minus Spearman correlation metric based on the average linkage method. Color scale represents the standardized expression values (Z-score) across samples. **b** Enriched gene ontology (GO) terms associated with diurnally rhythmic putative salivary effectors. Node color corresponds to the clade number in the heatmap (**a**). Source data and full statistical summary are provided in the Source Data file.

Figure 4. Aphid performance on wheat and artificial diet after silencing diurnally rhythmic salivary effectors. a Key salivary effector identification for functional analysis. Yellow and black dots represent diurnally rhythmic effectors with acrophases during the day and night. **b** Expression levels of C002 and E8696 in *R. padi* heads (n=3) and bodies (n=3, without heads and nymphs) are compared using a two-tailed Welch's *t*-test (C002: t=6.532, df=3.218, **p*=0.0059 and E8696: t=8.528, df=2.072, ***p*<0.0121). **c, d** Expression profiles of C002 (**c**) and E8696 (**d**) over a 24h period (n=3 per time point). Solid lines, boundaries, and whiskers of each box indicate the median, 25th, and 75th percentiles, and 1.5 interquartile ranges, respectively. Diurnal rhythmicity of C002 (*p*=0.008) and E8696 (*p*=0.001) was determined by Cosinor model. The curve line and shaded area represent the fitted periodic sinusoidal curve and 95% confidence band, respectively. **e** Kaplan-Meier survival curves and **f** fecundities of aphids on wheat plants after treatment with dsRNA C002 (dsC002, n=9), dsRNA E8696 (dsE8696, n=9), and dsRNA GFP (dsGFP, n=12, negative control). **g** Kaplan-Meier survival curves and **h** fecundities of aphids on diets after treatment with dsC002 (n=9), dsE8696 (n=11), and dsGFP (n=12). Significant differences in survivorship and fecundity were tested using a log-rank test with Benjamini-Hochberg adjustment and a repeated measures ANOVA with Dunn's multiple comparisons test, respectively (**p*<0.05, ***p*<0.01, ****p*<0.001, *****p*<0.0001). **i, j** The number of honeydew droplets produced per aphid after treatment with dsC002, dsE8696, and dsGFP on wheat plant (**i**, n=6 per treatment group) and diet (**j**, dsC002: n=6, dsE8696: n=8, and dsGFP: n=6). Yellow and black bars represent the mean (±SE) number of honeydew droplets produced at the end of each 12h day and night cycle for 4 days (Mann-Whitney test, **p*<0.05, ***p*<0.01, *****p*<0.0001). **k** Aphid feeding activity after treatment with dsE8696 (n=13) and dsGFP (n=15). Solid lines, boundaries, and whiskers indicate the median, 25th, and 75th percentiles and 1.5 interquartile ranges, respectively. Points indicate outliers. Asterisk(s) denote significant differences (Mann-Whitney test, E1: ***p*=0.0071 and E2: **p*=0.0195). Source data and full statistical summary are provided in the Source Data file.

Figure 5. a. Diurnal behavioral activities of *R. padi* on wheat plant and artificial diet. Five age-synchronized adult females were placed on a wheat leaf or diet under 12h:12h, light:dark cycles. The number of honeydew drops and nymphs produced by aphids was recorded at the end of each night and day for two days. Each experiment on wheat or diet contains a total of 10 biological replicates. **b. Diurnal time-course experiment.** Aphid samples were collected every four hours over a 24h day-night cycle (n = 3 per timepoint).

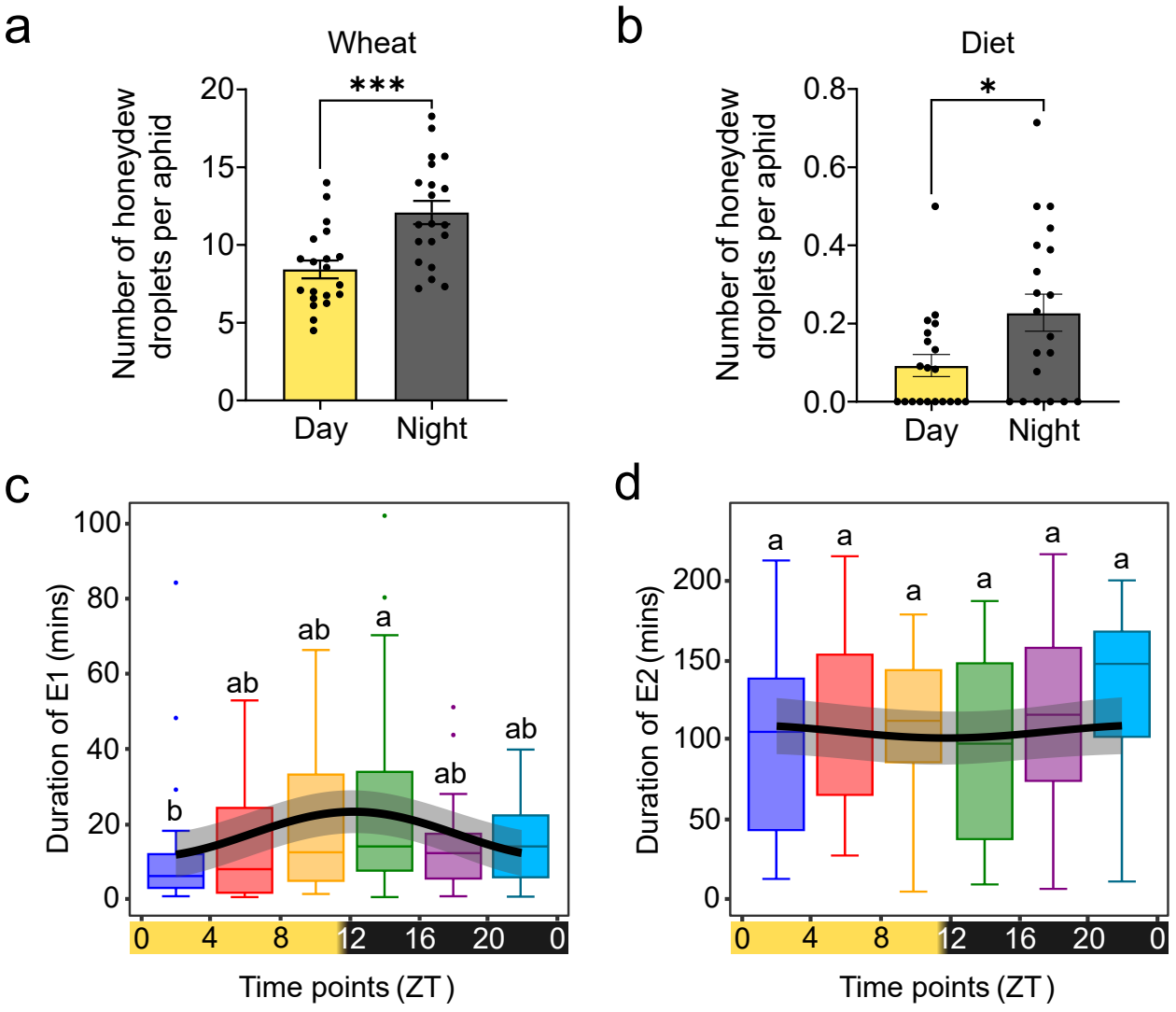
a
Wheat
***
Number of honeydew droplets per aphid
20
15
10
5
0
Day
Night
b
Diet
*
Number of honeydew droplets per aphid
0.8
0.6
0.4
0.2
0.0
Day
Night
c
Duration of E1 (mins)
100
80
60
40
20
0
b
ab
ab
a
ab
ab
0
4
8
12
16
20
0
Time points (ZT)
d
Duration of E2 (mins)
200
150
100
50
0
a
a
a
a
a
a
0
4
8
12
16
20
0
Time points (ZT)

Figure 1

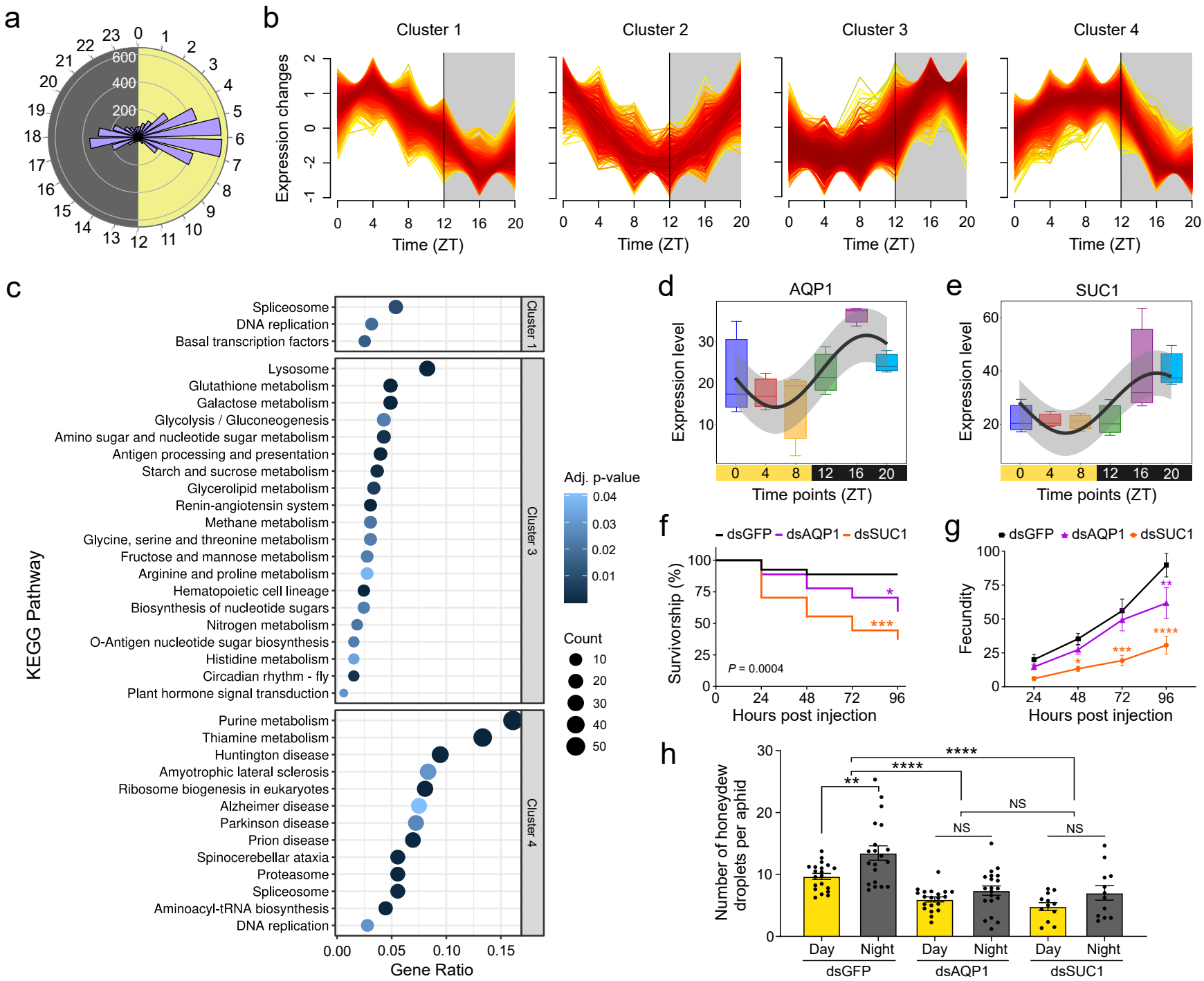
a
b
Cluster 1
Cluster 2
Cluster 3
Cluster 4
Expression changes
Time (ZT)
c
KEGG Pathway
Spliceosome
DNA replication
Basal transcription factors
Lysosome
Glutathione metabolism
Galactose metabolism
Glycolysis / Gluconeogenesis
Amino sugar and nucleotide sugar metabolism
Antigen processing and presentation
Starch and sucrose metabolism
Glycerolipid metabolism
Renin-angiotensin system
Methane metabolism
Glycine, serine and threonine metabolism
Fructose and mannose metabolism
Arginine and proline metabolism
Hematopoietic cell lineage
Biosynthesis of nucleotide sugars
Nitrogen metabolism
O-Antigen nucleotide sugar biosynthesis
Histidine metabolism
Circadian rhythm - fly
Plant hormone signal transduction
Purine metabolism
Thiamine metabolism
Huntington disease
Amyotrophic lateral sclerosis
Ribosome biogenesis in eukaryotes
Alzheimer disease
Parkinson disease
Prion disease
Spinocerebellar ataxia
Proteasome
Spliceosome
Aminoacyl-tRNA biosynthesis
DNA replication
Gene Ratio
Adj. p-value
Count
d
AQP1
Expression level
Time points (ZT)
e
SUC1
Expression level
Time points (ZT)
f
dsGFP
dsAQP1
dsSUC1
Survivorship (%)
P = 0.0004
Hours post injection
g
dsGFP
dsAQP1
dsSUC1
Fecundity
Hours post injection
h
Number of honeydew droplets per aphid
Day
Night
dsGFP
dsAQP1
dsSUC1
NS

Figure 2

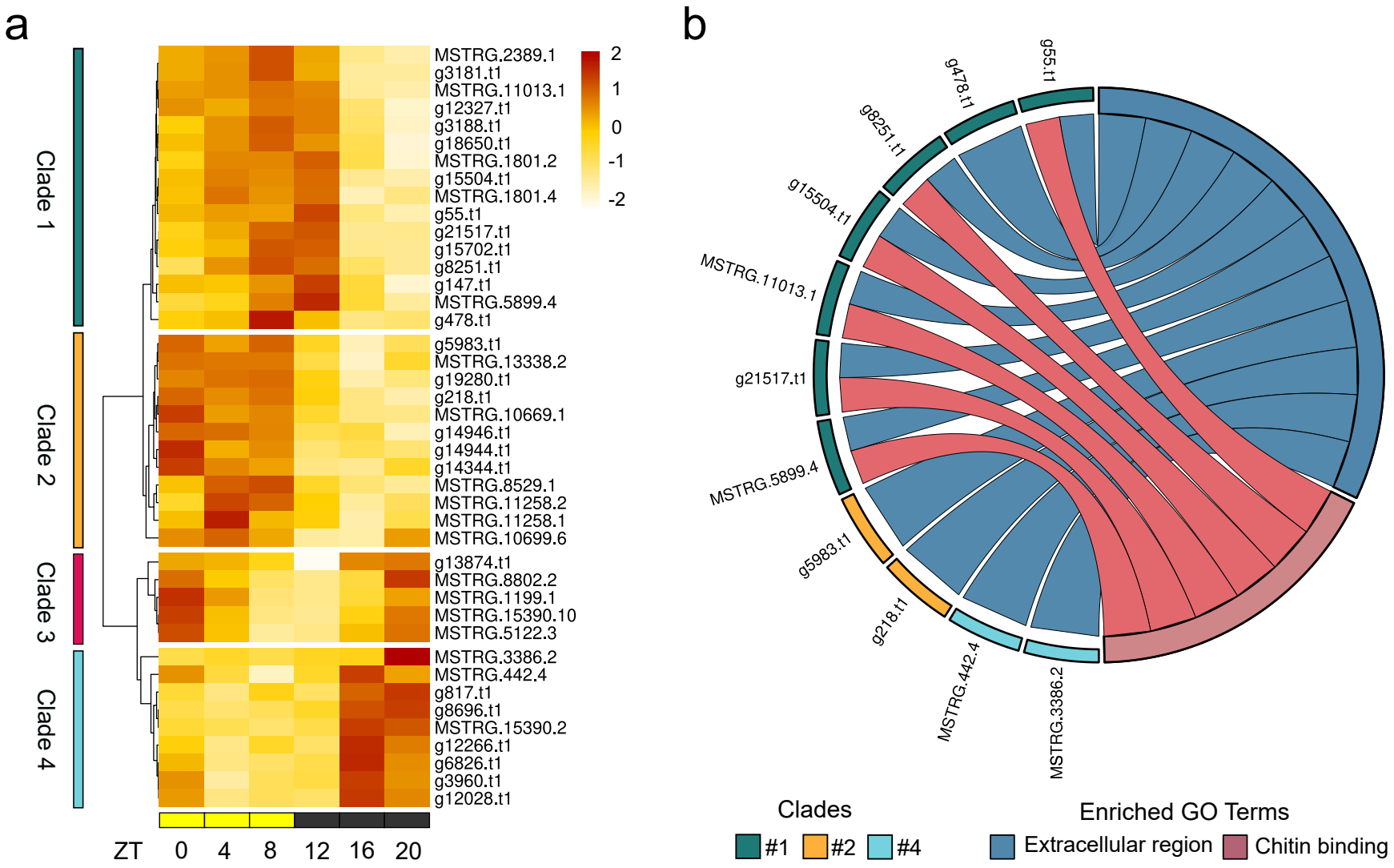
a
Clade 1
Clade 2
Clade 3
Clade 4
MSTRG.2389.1
g3181.t1
MSTRG.11013.1
g12327.t1
g3188.t1
g18650.t1
MSTRG.1801.2
g15504.t1
MSTRG.1801.4
g55.t1
g21517.t1
g15702.t1
g8251.t1
g147.t1
MSTRG.5899.4
g478.t1
g5983.t1
MSTRG.13338.2
g19280.t1
g218.t1
MSTRG.10669.1
g14946.t1
g14944.t1
g14344.t1
MSTRG.8529.1
MSTRG.11258.2
MSTRG.11258.1
MSTRG.10699.6
g13874.t1
MSTRG.8802.2
MSTRG.1199.1
MSTRG.15390.10
MSTRG.5122.3
MSTRG.3386.2
MSTRG.442.4
g817.t1
g8696.t1
MSTRG.15390.2
g12266.t1
g6826.t1
g3960.t1
g12028.t1
2
1
0
-1
-2
ZT 0 4 8 12 16 20
b
g55.t1
g478.t1
g8251.t1
g15504.t1
MSTRG.11013.1
g21517.t1
MSTRG.5899.4
g5983.t1
g218.t1
MSTRG.442.4
MSTRG.3386.2
Clades
#1
#2
#4
Enriched GO Terms
Extracellular region
Chitin binding

Figure 3

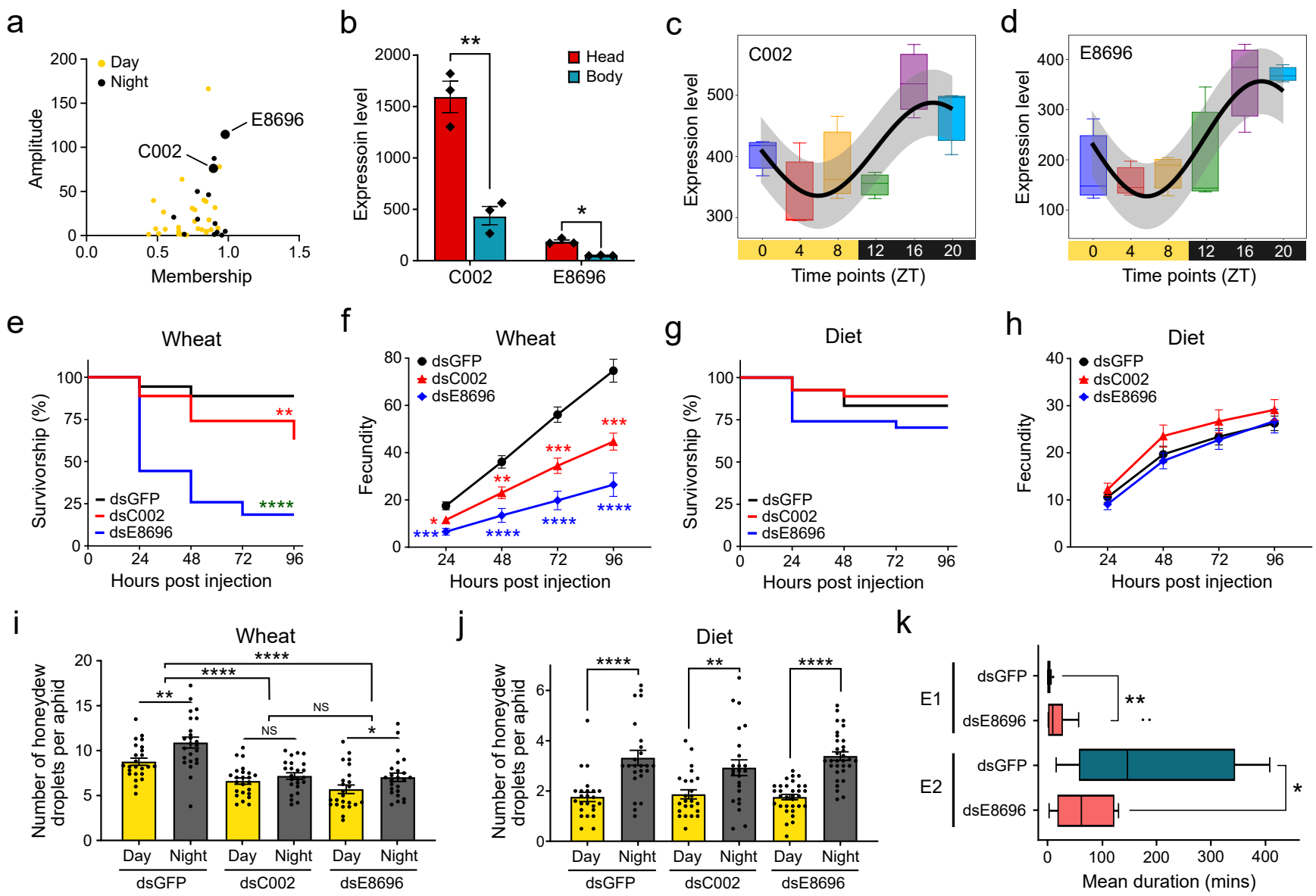
a
Day
Night
Amplitude
Membership
E8696
C002
b
Head
Body
Expressoin level
C002
E8696
c
C002
Expression level
Time points (ZT)
d
E8696
Expression level
Time points (ZT)
e
Wheat
Survivorship (%)
dsGFP
dsC002
dsE8696
Hours post injection
f
Wheat
Fecundity
dsGFP
dsC002
dsE8696
Hours post injection
g
Diet
Survivorship (%)
dsGFP
dsC002
dsE8696
Hours post injection
h
Diet
Fecundity
dsGFP
dsC002
dsE8696
Hours post injection
i
Wheat
Number of honeydew droplets per aphid
Day
Night
dsGFP
dsC002
dsE8696
NS
j
Diet
Number of honeydew droplets per aphid
Day
Night
dsGFP
dsC002
dsE8696
k
E1
E2
dsGFP
dsE8696
Mean duration (mins)

Figure 4

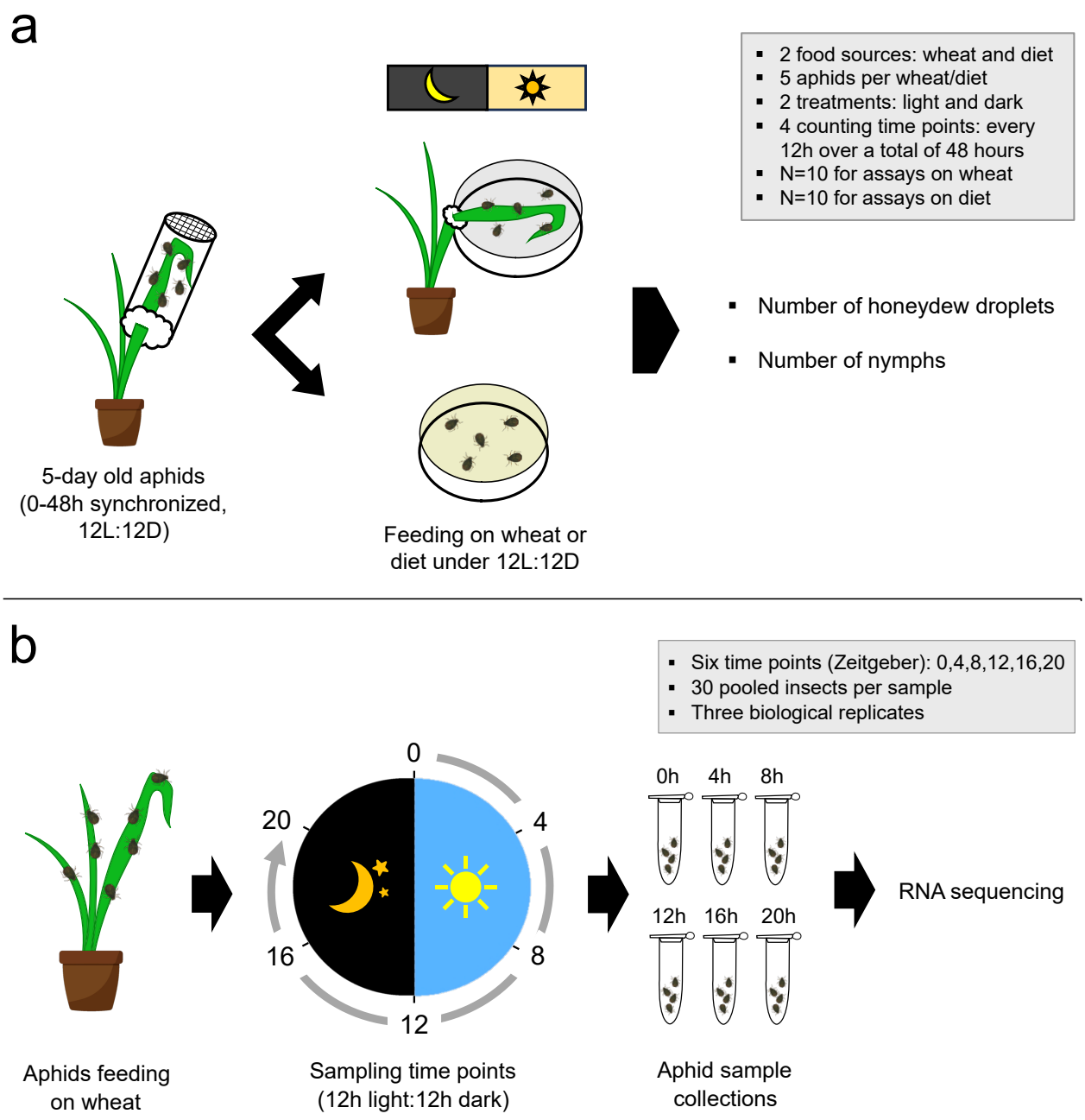
a
2 food sources: wheat and diet
5 aphids per wheat/diet
2 treatments: light and dark
4 counting time points: every 12h over a total of 48 hours
N=10 for assays on wheat
N=10 for assays on diet
Number of honeydew droplets
Number of nymphs
5-day old aphids (0-48h synchronized, 12L:12D)
Feeding on wheat or diet under 12L:12D
b
Six time points (Zeitgeber): 0,4,8,12,16,20
30 pooled insects per sample
Three biological replicates
0
4
8
12
16
20
0h
4h
8h
12h
16h
20h
RNA sequencing
Aphids feeding on wheat
Sampling time points (12h light:12h dark)
Aphid sample collections

Figure 5